ORIGINAL PAPER

Mechanochemical synthesis of Na-β/β″-Al$_2$O$_3$

Jiu Lin · Zhaoyin Wen · Xiuyan Wang · Shufeng Song · Yu Liu

Abstract Na-β/β″-alumina powders were synthesized by a mechanochemical processing. The influences of mechanical activation in the phase composition and microstructure of the final powders were investigated. Fine Na-β/β″-alumina powders were obtained at a lower temperature than that of a conventional solid-state reaction processing. The mechanism of the mechanical activation was studied. It was found that mechanical activation greatly affected the calcining process and phase composition of the precursory powders.

Keywords Beta alumina · Sodium sulfur battery · Mechanochemical · Microstructure

Introduction

Na-beta–Al$_2$O$_3$ has been used as solid electrolyte in the sodium sulfur battery and zebra battery because of its high Na$^+$ conductivity [1]. Na-beta–Al$_2$O$_3$ is known to be a nonstoichiometric oxide, assigned the formula Na$_2$O·x-Al$_2$O$_3$ (5≤x≤11). Most research work about Na-beta–Al$_2$O$_3$ focused on the Na-β–Al$_2$O$_3$ and Na-β″-Al$_2$O$_3$, assigned the formula Na$_2$O·11Al$_2$O$_3$ and Na$_2$O·5.33Al$_2$O$_3$ respectively [2, 3]. The conventional synthetic method for Na-beta–Al$_2$O$_3$ is the solid-state reaction at high temperature usually between 1,200 °C–1,700 °C, using alpha alumina and sodium compound as the raw materials. The loss of Na component at high temperature brings difficulties to the stoichiometric control of the final powders and ceramics. Furthermore, the extreme grain growth at a high temperature is an obstacle for the fabrication of Na-beta–Al$_2$O$_3$ electrolytes with preferable electrochemical performance. To overcome these problems, many novel methods have been developed for preparing Na-beta-alumina (SBA) powders and ceramics in recent years. Magnesium compensated Na-beta-alumina with different compositions were synthesized through a rapid-solution combustion route using stoichiometric amounts of metal nitrates and urea by Mathews [4]. The use of microwave as the heating source for the preparation of SBA was attempted by Subasri et al [5]. It was demonstrated in their investigation that Na-β–alumina as well as Na-β″–alumina could be processed using microwaves in a short period of time to produce ceramic bodies with a relative density greater than 95%. Subsequently, Subasri investigated the factors assisted a one-step synthesis cum calcing of SBA by microwaves [6]. The presence of structurally bonded H$_2$O molecules in the mullite-like-alumina and the similarity of its structure with Na-β/β″–alumina were concluded as the reasons for its microwave activity at low temperatures. A sol–gel route was also applied to prepare SBA powders by Sartori et al. [7]. It was found in their study that the fine β-alumina powder obtained by the sol–gel processing made it possible to sinter dense pellets at the temperature as low as 1,400 °C. Moreover, the polycrystalline β-alumina pellets showed good ionic conductive performance.

Mechanochemical method is an efficient and low-cost approach to prepare powders with fine particle size and high sintering activity [8, 9]. Therefore, it is possible to reduce the calcining temperature and energy consumption in the preparation of Na-beta–alumina ceramics with a mechanochemical processing. In this paper, fine Na-β/β″–Al$_2$O$_3$ powders were prepared by the mechanochemical processing. The difference in phase and microstructure between powders obtained by the mechanochemical pro-

J. Lin · Z. Wen (✉) · X. Wang · S. Song · Y. Liu
Shanghai Institute of Ceramics, Chinese Academy of Sciences,
1295 DingXi Road,
Shanghai 200050, People's Republic of China
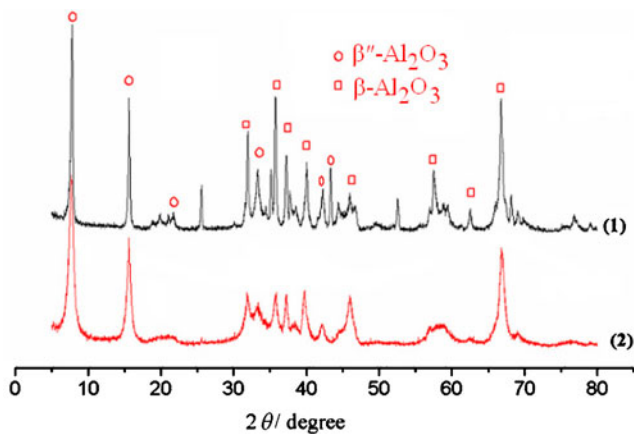e-mail: zywen@mail.sic.ac.cn

Fig. 1 XRD patterns of powders prepared by: (*1*) MA processing and (*2*) conventional solid state reaction

cessing and the conventional solid-state reaction was investigated. The mechanism of the mechanochemical fabrication of Na-β/β''–Al$_2$O$_3$ was discussed. The influence of the mechanochemical processing in the conductive performance of the ceramics was also examined.

Experimental

Sodium carbonate and aluminum hydroxide were used as the sodium and aluminum resource respectively. A stoichiometric amount of sodium resource and aluminum

resource with the cationic ratio of Na/Al=1:7.5 were mixed by planetary milling with ethanol as the dispersion medium. The slurry was dried at 50 °C to volatilize the ethanol. Then, the mixture was mechanically activated at a high energy mechanical mixer (pulverisette 5, FRITSCH, Germany), using alumina as the container and milling balls. The powders mechanically activated were then heat-treated at the temperature in the range of 1,000 °C–1,200 °C. The sample for contrast was directly calcined at the same temperature without mechanical activation (MA).

Phases of mechanically activated powders and the powders after heat treatment were determined by X-ray diffraction (XRD, Rigaku RAD-C). Microstructure of the final powders was characterized by Electron Probe Micro Analysis (EPMA, JEOL.JXA-8100). Influences of mechanical activation in the compositions and calcining thermodynamic process of precursors were investigated with infrared spectrum (FTIR, TESSOR 27, Bruker) and differential scanning calorimetry (TG-DSC, STA 409PC, NETZSCH).

The powders obtained from the mechanochemical processing and the conventional solid-state reaction were shaped to disks (around 12 mm in diameter, 2 mm in thickness) by isostatic pressing at 200 MPa. The green bodies were sintered at 1,600 °C for 20 min and annealed at 1,500 °C for 2 h. The opposing faces of the sintered pellets were coated with gold electrode by vacuum sputtering. The ionic conductivity of the ceramics was obtained from the AC impedance plots examined on a frequency response analyzer (Autolab AUT83601) over a

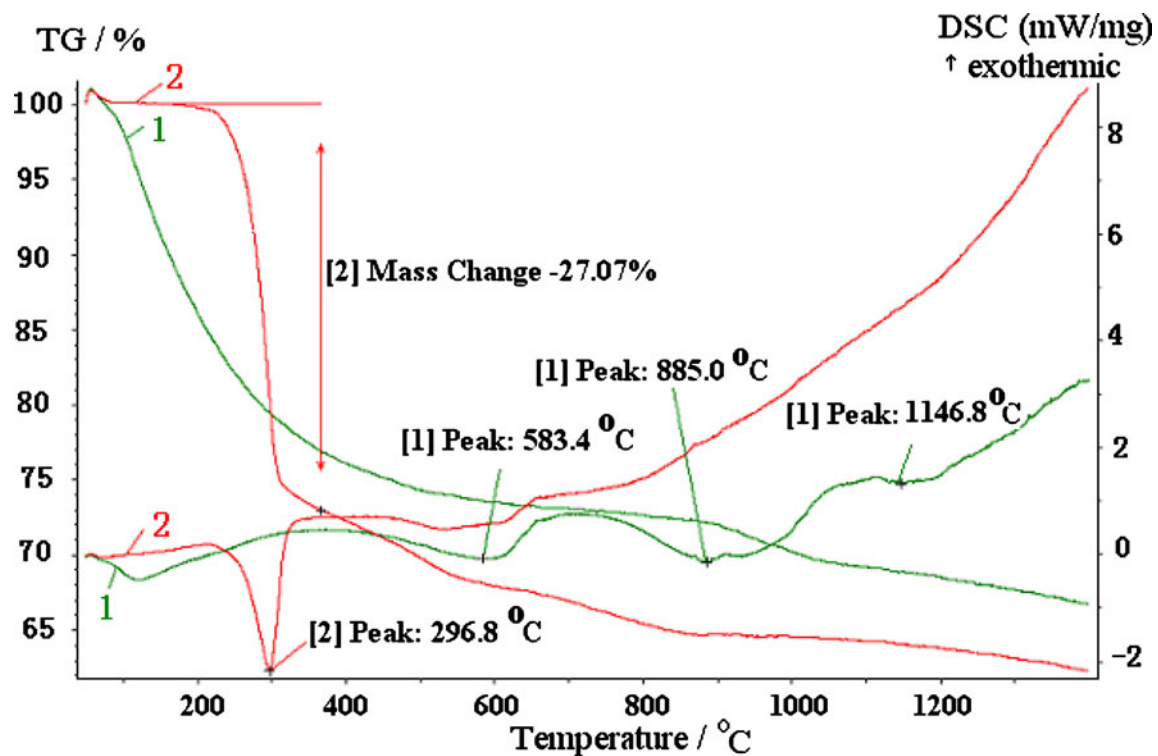**Fig. 2** EPMA graphs of calcinated powders: **a**, **b** no MA and **c**, **d** with MA
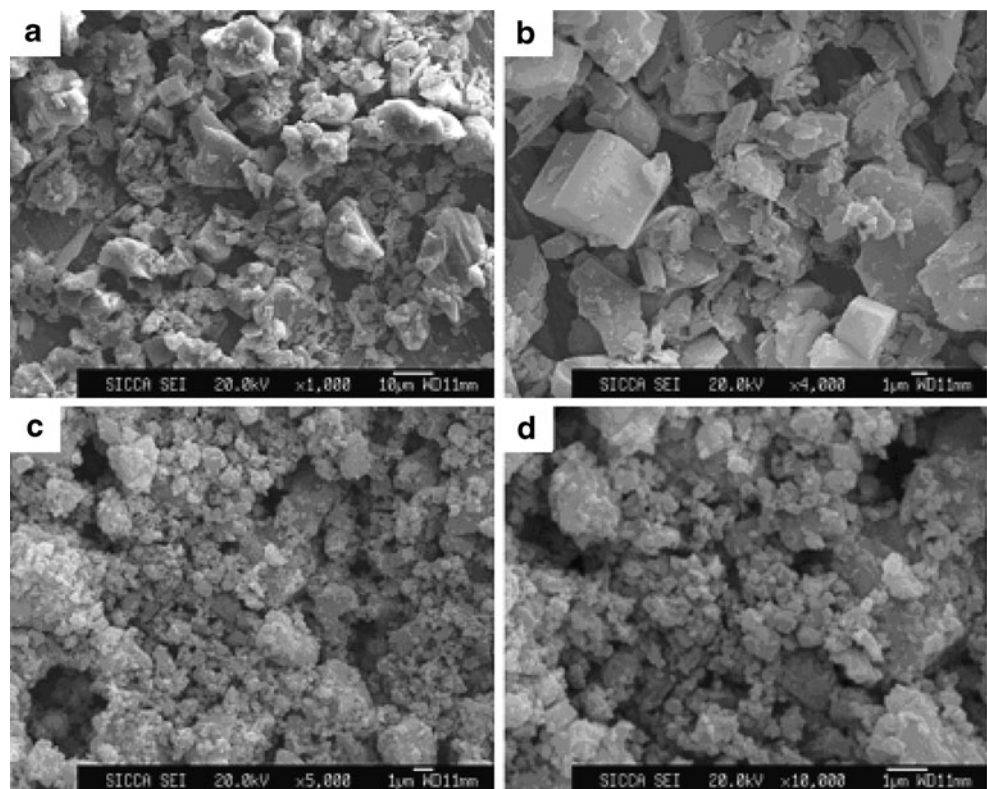
Fig. 3 TG-DSC curves of powders (*1*) with 60 min MA and (*2*) no MA

frequency range of 100 Hz to 1 MHz and a temperature range of 10 °C–350 °C. Spectra were collected in potentiostatic mode with signal amplitude of 10 mV.

Results and discussion

Influence of MA in phase and microstructure

To detect the influence of MA in the phase composition of the final powders, XRD patterns of the samples calcined at 1,200 °C for 2 h from precursors with 60 minutes' MA and without MA were tested and shown in Fig. 1. It can be seen that the powders prepared by the mechanochemical processing consisted of both β''-Al_2O_3 and β-Al_2O_3. The diffraction peaks of the MA-synthesized powders were much sharper than those of the powders without MA, indicating the better crystallization of the powders obtained by the MA processing than the powders prepared without MA processing. Therefore, it is feasible to obtain the Na-β/β''–Al_2O_3 phase by the mechanochemical processing at a lower calcining temperature than that of the conventional solid reaction processing.

The effect of MA in the microstructure of the calcined powders was observed by EPMA. Figure 2 displays the EPMA graphs of powders obtained at 1,200 °C. As shown in Fig. 2a, b, powders directly calcined from precursors without MA had an average grain size of 2–3 μm. The grain size of powders obtained at the same temperature

after MA (Fig 2cd) decreased to submicron dimension. What's more, the powders prepared by the MA processing displayed more uniform grain size with less aggregations than powders prepared without MA. Therefore, the mechanochemical processing helped prepare fine Na-β/β''–Al_2O_3 powders at a lower temperature.

Mechanism of mechanical activation

As discussed above, mechanochemical processing had strong influence in the phase and microstructure of the
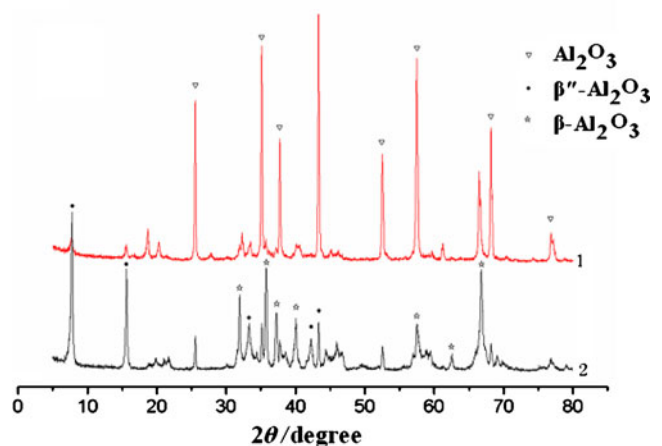

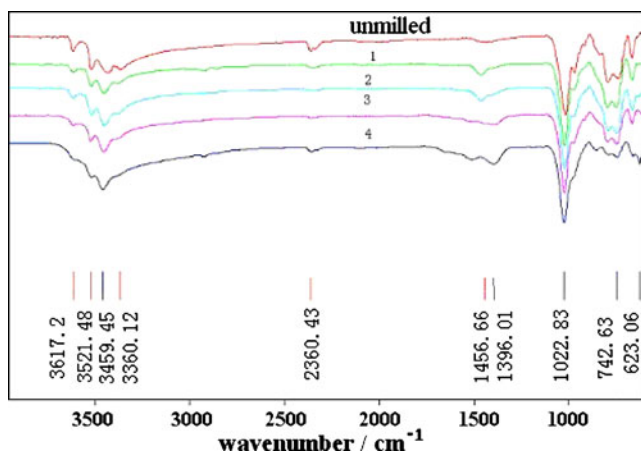**Fig. 4** XRD patterns of MA-powders calcined for 2 h at (*1*) 1,000 °C and (*2*) 12,000 °C

Fig. 5 FTIR spectrums of powders without MA and after MA for (*1*) 5 min, (*2*) 10 min, (*3*) 30 min, and (*4*) 60 min

final products. The influences of MA in calcining process, compositions, and phases of precursory powders were then investigated.

TG-DSC curves of the precursory powders after MA and without MA are displayed in Fig. 3. The TG-DSC graph shows remarkable influence of MA in the calcining thermodynamics of the precursory powders. For the powders without MA, a drastic mass loss was found in the temperature range of 200 °C–300 °C on the TG curve, associated with a sharp endothermic peak at 296.8 °C on the DSC curve. The aluminum hydroxide in the mixture powders was apt to decompose into alumina and water vapor between 200 °C–300 °C. When all aluminum hydroxide in the mixture (with mole ratio of $Na_2CO_3/Al(OH)_3=1:15$) decompose into alumina, the theoretical mass loss should be around 31%. The experimental mass loss was around 27%, a little less than the theoretical data mainly due to the incomplete decomposition of aluminum

hydroxide. No clear phase forming DSC peaks were found for the powders without MA. The main difference between the TG-DSC curves of the precursory powders with MA and without MA existed in the temperature range of 500 °C–1,200 °C. Three endothermic peaks were found on the DSC curve of the powders with MA. The endothermic peak at 583.4 °C may be attributed to the decomposition of products activated during MA. The endothermic peak at 885 °C was closely followed by a mass loss. This endothermic peak could be attributed to the melting of sodium carbonate in the mixture.

The phase composition of the powders calcined at 1,000 °C for 2 h shown in Fig. 4 proved that the weight loss around 1,000 °C could be attributed to the formation of a small amount of Na-β''–Al_2O_3 from alumina and molten sodium carbonate. As shown in Fig. 4, the powders calcined at 1,200 °C for 2 h comprised of Na-β/β''–Al_2O_3, suggesting that the weight loss and endothermic peak at 1,100 °C–1,200 °C stand for the formation of Na-β/β''–Al_2O_3 phases.

From the calcining thermodynamic analysis, it can be deduced that the MA processing enhanced the reaction activity of precursory mixture of sodium carbonate and aluminum hydroxide. As a consequence, the influences of MA in composition and phases of the precursory powders were investigated.

The FTIR absorption spectra of the precursory powders after being mechanically activated for different time are shown in Fig. 5. It was discovered that, when the MA time was increased, the absorption peak around 1,400 cm^{-1} became weak. At the same time, the absorption peak around 1,500 cm^{-1}, corresponding to the absorption of Na_2CO_3, appeared. The shoulder peaks between 3,650 cm^{-1} and 3,500 cm^{-1} ascribed to the characteristic absorption band of O-H bond became weak. Therefore, it can be

Fig. 6 XRD patterns of powders after MA for (*1*) 3 min, (*2*) 30 min, and (*3*) 60 min
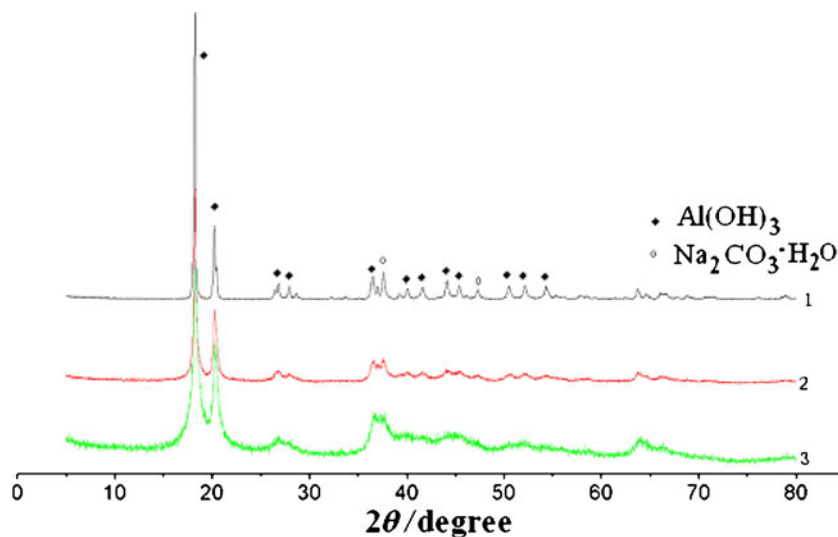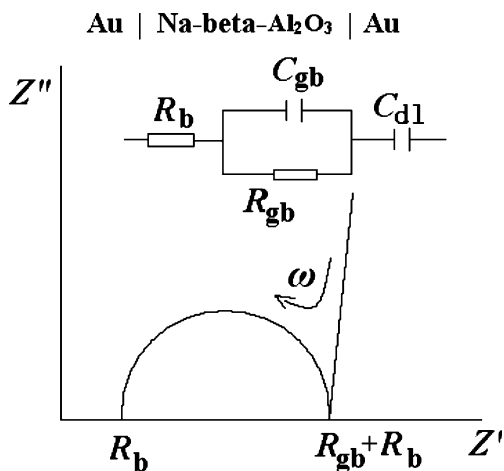
Fig. 7 Equivalent circuit and theoretical impedance complex plane graph of the cells tested

deduced that MA brought influences to Na_2CO_3 and O-H bonds. These influences can also be seen in phase composition of powders after being mechanically activated for different time as shown in Fig. 6. It was found in the XRD patterns that diffraction peaks of Na_2CO_3 were firstly transferred to those of $Na_2CO_3 \cdot H_2O$ and then widened. Besides, strong diffraction peaks of $Al(OH)_3$ were also widened. Some weak peaks of $Al(OH)_3$ even disappeared. Therefore, the MA processing transferred crystalline Na_2CO_3 and $Al(OH)_3$ to amorphous state, enhancing the reaction activity of the precursory powders. Lithium aluminum layered double hydroxides (Li-Al LDHs) were found in the mixture of lithium carbonate and aluminum hydroxide during mechanochemical syn-

thesis of $LiAlO_2$ by Kharlamova and Mitrofanova [10]. It is worth investigating further if the sodium aluminum layered double hydroxides with the similar structure of Li-Al LDHs are possibly formed in the mechano-chemical processing.

Influence in ionic conductivity

To determine the influence of the MA processing in the conductive performance of the ceramics, the AC impedance spectra of the cells with the polycrystalline Na-β/β″–Al_2O_3 ceramics as electrolyte and gold as blocking electrodes were examined. The cell obtained from the MA processing was 1.15 mm in diameter and 0.18 mm in thickness. The cell obtained from the conventional solid state reaction was 1.16 mm in diameter and 0.14 mm in thickness. The equivalent circuit and theoretical Nyquist plot is displayed in Fig. 7 [11]. As shown, the bulk resistance (R_b) and grain boundary resistance (R_{gb}) can be read in the impedance complex plane graph when they have different response frequency range. But, the real spectra for Na-β/β″–Al_2O_3 ceramics were not so readable. At the low temperature (<200 °C), it was possible to separate out the semi-cycle part and the line part as shown in Fig. 8. The semi-cycle part was substituted by some dots close to the Z' axis when the temperature was higher than 200 °C because the grain boundary or intergranular resistance became negligible at above 200 °C [12]. Figure 9 displays the typical impedance spectra for the Na-β/β″–Al_2O_3 ceramics at high temperature, in which the total resistance of the electrolyte was obtained approximately from the beginning of the line part.
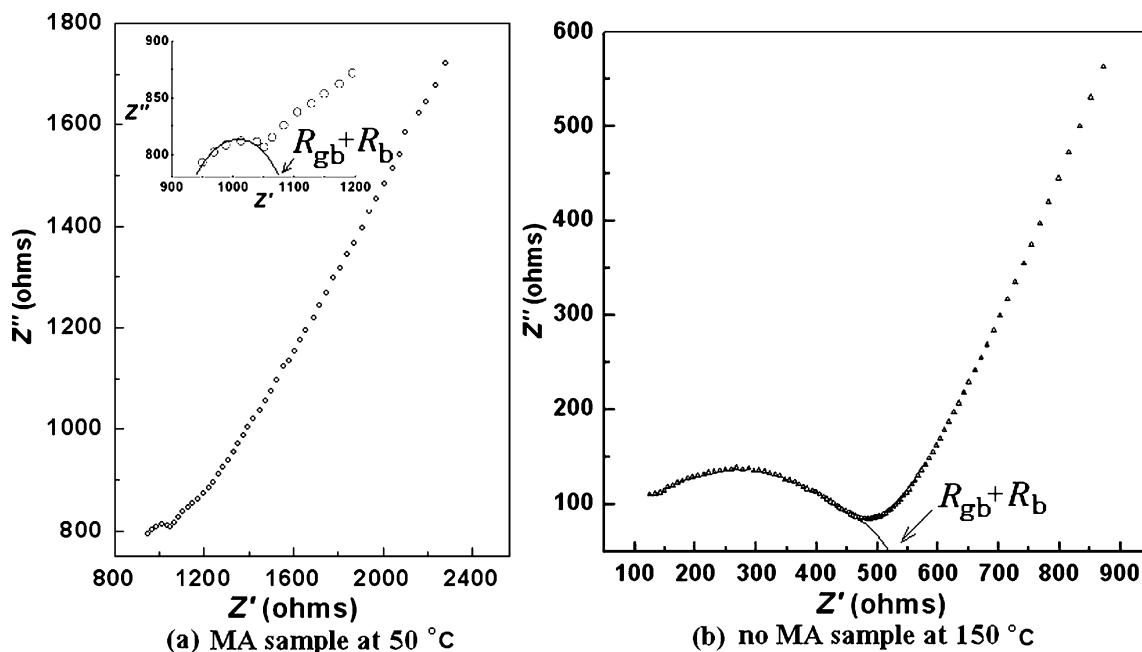

Fig. 8 AC impedance of Na-β/β″–Al_2O_3 at low temperature

The conductivities of the ceramics at different temperatures were calculated from the total resistance and sizes of the disks according to Eq. 1 and shown in Table 1.

$$\sigma = \frac{d}{RS} \qquad (1)$$

where σ is the conductivity, d and S are the thickness and round surface area of the disk, respectively, and R is the total resistance (a sum of bulk and grain boundary resistance). The temperature dependence of the conductivity of beta-alumina obeys the Arrhenius law expressed by Eq. 2 [13].

$$\sigma T = \sigma_o \exp\left(\frac{-E}{kT}\right) \qquad (2)$$

where T is the temperature, σ_o is a parameter determined by the crystal structure, E is the activation energy, and k is the Boltzman constant. Therefore, the values of the activation energy of the electrolytes were obtained from the plots of ln (σT) against 1,000/T shown in Fig. 10.

It can be found in Table 1 and Fig. 10 that the ceramics obtained by the MA processing had higher conductivity in all the temperature range tested than specimen obtained by the no MA processing. The results of the activation energy in Fig. 10 also show advantage of the MA processing over the conventional high temperature processing. The better conductivity of the ceramics obtained from the MA processing can be explained by its higher density than that of specimen obtained by the conventional solid state reaction. The difference in the density was attributed to the good sintering activity of the powders obtained by the MA processing. The conductivity of the Na-β/β''–Al$_2$O$_3$ ceramics obtained by the MA processing in this study was much higher than that of the ceramics prepared by Sartori et al. with a sol–gel processing (10^{-4} order at 400 °C) [7] but not so good as the polycrystalline Na-β''–Al$_2$O$_3$ prepared

by Virkar et al. (0.2–0.4 Ω^{-1}cm^{-1} at 300 °C) [14]. The composition of the Na-β/β''–Al$_2$O$_3$ ceramics should have important influence in the conductivity. The increase of the ratio of the β'' phase and the homogeneity of the final powders should be further investigated for the real application of the MA processing for the production of Na-beta–Al$_2$O$_3$ electrolyte.

Table 1 Conductivities of ceramics at different temperature

T (K)	$\sigma \times 10,000$ (Ω^{-1}cm^{-1})	
	MA sample	No MA sample
298	0.80	0.32
323	2.32	0.43
373	3.80	1.91
423	20.38	4.25
473	65.33	31.80
523	127.39	79.60
573	195.98	127.00
623	254.78	159.00

Summary

Na-β/β''–Al$_2$O$_3$ powders were prepared by a mechanochemical process. The powders obtained at a low temperature showed more favorable microstructure than that obtained by a conventional high temperature solid reaction process. Precursors with high thermodynamic activity were obtained by mechanical activation. Crystalline sodium carbonate and aluminum hydroxide were partly transferred to amorphous state during mechanical activation, which enhanced the reaction activity of precursory powders. The
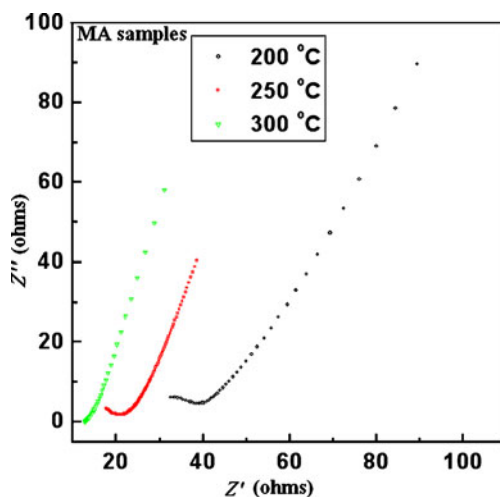

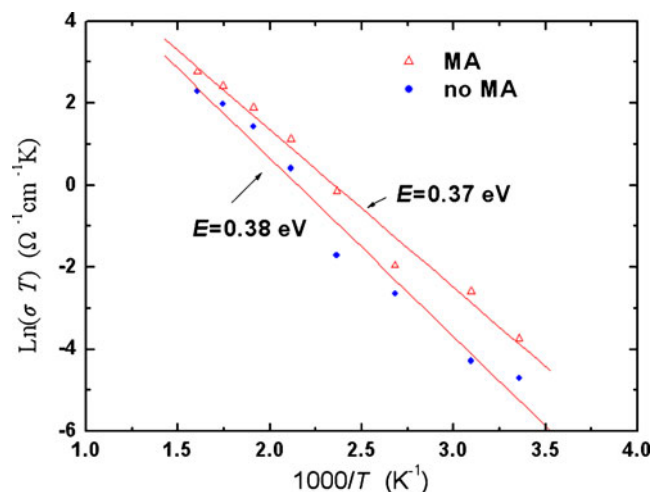**Fig. 9** AC impedance of Na-β/β''–Al$_2$O$_3$ at high temperature

Fig. 10 Arrhenius plots of specimens obtained from the MA processing and no MA processing

ceramics obtained by the MA processing displayed better conductive performance than that prepared by the conventional solid state reaction.

References

1. Sudworth JL (1996) High-temperature battery systems. Philos Trans R Soc Lond Ser A: Math Phys Eng Sci 354:1595–1611
2. Yamaguch G, Suzuki K (1968) On the structures of alkali polyaluminates. B Chem Soc Jpn 41:93–99
3. Dell RM, Moseley PT (1981) Beta-alumina electrolyte for use in sodium-sulfur batteries. 1. Fundamental properties. J Power Sources 6:143–160
4. Mathews T (2000) Solution combustion synthesis of magnesium compensated sodium-beta-aluminas. Mat Sci Eng B-Solid 78:39–43
5. Subasri R, Mathews T, Sreedharan OM, Raghunathan VS (2003) Microwave processing of sodium beta alumina. Solid State Ionics 158:199–204
6. Subasri R (2004) Investigations on the factors assisting a one-step synthesis cum sintering of sodium beta alumina using microwaves. Mat Sci Eng B-Solid 112:73–78
7. Sartori S, Martucci A, Muffato A, Guglielmi M (2004) Sol–gel synthesis of Na + beta-Al2O3 powders. J Eur Ceram Soc 24:911–914
8. Tsuzuki T, McCormick PG (2004) Mechanochemical synthesis of nanoparticles. J Mater Sci 39:5143–5146
9. Borjas SE, Yamamoto K, Muramatsu A (2008) Synthesis of Ti-beta via mechanochemical route. J Mater Sci 43:2367–2371
10. Kharlamova OA, Mitrofanova RP, Isupov VP (2007) Mechanochemical synthesis of fine-particle gamma-LiAlO2. Inorg Mater 43:645–650
11. Xiang LZ, Kun GZ, Wen SC, Chun LS (1983) Fast ionic conductors. Shanghai Publish House of Science and Technology, Shanghai
12. Hooper A (1977) Study of electrical-properties of single-crystal and polycrystalline Beta-alumina using complex plane analysis. Journal of Physics D-Applied Physics 10:1487–1496
13. Sudworth JL, Tilley AR (1985) The sodium sulfur battery. Cambridge University Press, London
14. Virkar AV, Miller GR, Gordon RS (1978) Resistivity microstructure relations in lithia-stabilized polycrystalline beta"–alumina. J Am Ceram Soc 61:250–252